Quarterly Technical Report

Selected Energy Epitaxial Deposition and Low Energy Electron Microscopy of AlN, GaN and SiC Thin Films

Supported under Grant #N00014-95-1-0122
Office of the Chief of Naval Research
Report for the period 7/1/96–9/30/96

R. F. Davis, H. H. Lamb† and I. S. T. Tsong*,
E. Bauer*, E. Chen†, R. Chilukuri†, R. B. Doak*, J. L. Edwards*,
N. Freed*, J. Fritsch, S. Horch*, C. Linsmeier*, M. Meloni*,
K. E. Schmidt*, V. Torres,* and S. Zhang
Materials Science and Engineering Department
†Chemical Engineering
North Carolina State University
Campus Box 7907
Raleigh, NC 27695-7907
and
*Department of Physics and Astronomy
Arizona State University
Tempe, AZ 85287-1504

September, 1996

DISCLAIMER NOTICE

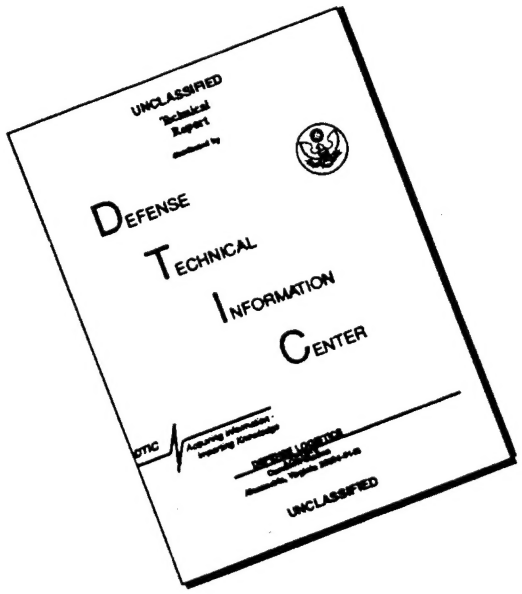

THIS DOCUMENT IS BEST QUALITY AVAILABLE. THE COPY FURNISHED TO DTIC CONTAINED A SIGNIFICANT NUMBER OF PAGES WHICH DO NOT REPRODUCE LEGIBLY.

REPORT DOCUMENTATION PAGE

Form Approved
OMB No. 0704-0188

1. AGENCY USE ONLY *(Leave blank)*	2. REPORT DATE	3. REPORT TYPE AND DATES COVERED
	September, 1996	Quarterly Technical 7/1/96–9/30/96

4. TITLE AND SUBTITLE
Selected Energy Epitaxial Deposition and Low Energy Electron Microscopy of AlN, GaN, and SiC Thin Films

5. FUNDING NUMBERS
1213801---01
312
N00179
N66020
4B855

6. AUTHOR(S)
R. F. Davis, H. H. Lamb and I. S. T. Tsong

7. PERFORMING ORGANIZATION NAME(S) AND ADDRESS(ES)
North Carolina State University
Hillsborough Street
Raleigh, NC 27695

8. PERFORMING ORGANIZATION REPORT NUMBER
N00014-95-1-0122

9. SPONSORING/MONITORING AGENCY NAMES(S) AND ADDRESS(ES)
Sponsoring: ONR, Code 312, 800 N. Quincy, Arlington, VA 22217-5660
Monitoring: Administrative Contracting Officer, Regional Office Atlanta
Regional Office Atlanta, 101 Marietta Tower, Suite 2805
101 Marietta Street
Atlanta, GA 30323-0008

10. SPONSORING/MONITORING AGENCY REPORT NUMBER

11. SUPPLEMENTARY NOTES

12a. DISTRIBUTION/AVAILABILITY STATEMENT
Approved for Public Release; Distribution Unlimited

12b. DISTRIBUTION CODE

13. ABSTRACT *(Maximum 200 words)*

Within the multicenter tight-binding formalism, experimentally determined structural parameters and phonon frequencies of GaN and AlN in both the zinc-blende and the wurtzite phase have been reproduced with an accuracy that is similar to highly converged *ab initio* calculations. Thus, a reliable basis that allows realistic molecular-dynamics simulations for surface structure calculations and the investigation of the collision dynamics of small molecules on surfaces now exists. Different approaches were attempted to obtain clean, flat, and scratch-free 6H-SiC(0001) substrates for the epitaxial growth of nitride films. LEEM images show that the *ex situ* high-temperature etching treatment by NASA Lewis produced satisfactory surfaces. An *in situ* etching/cleaning scheme involving the use of silane gas (SiH_4) also produced flat terraces and atomic steps on the 6H-SiC(0001) surface as imaged by STM. The first GaN growth experiments using dual seeded supersonic beams of ammonia and triethylgallium were performed. The initial experiments using hydrogen-passivated Si(100) substrates at 600°C were not successful. Growth experiments are continuing using sapphire(0001) substrates. Successful *ex situ* cleaning and *in situ* remote plasma nitridation of GaP(100) substrates were examined using AES, XPS and LEED. UV/O_3 cleaning followed by etching in either hydrochloric or phosphoric acid was effective in removing C and O contamination from GaP. Subsequent UHV annealing at 800°C had little effect on the surface composition. *In situ* exposure to a remote N_2 plasma at 200°C for 5 min was effective at removing residual carbon and converting the surface layer to GaN. Deposition of AlN layers on Si(100) has been accomplished with a seeded supersonic molecular beam under conditions suitable for observation in the Low Energy Electron Microscope (LEEM). Alignment of the various components in the two low-energy ion-beam systems is ongoing. Ion beams of Ar^+, N_2^+, N^+, and C^+ have been obtained at energies of 10-20 eV with current densities ~200 nA cm^{-2}, corresponding to a deposition rate of ~10^{-3} MLs^{-1}. The energy distribution of the Ar^+ ions at 20 eV measured by the electrostatic energy analyzer (ESA) are illustrated.

14. SUBJECT TERMS
III-V nitrides, tight-binding formalism, zinc blende, wurtzite, molecular dynamics, 6H-SiC, cleaning supersonic beams, low energy electron microscope, ammonia, triethylgallium, *ex situ* cleaning, GaP, etching, AlN, ion beams, energy distribution

15. NUMBER OF PAGES
27

16. PRICE CODE

17. SECURITY CLASSIFICATION OF REPORT	18. SECURITY CLASSIFICATION OF THIS PAGE	19. SECURITY CLASSIFICATION OF ABSTRACT	20. LIMITATION OF ABSTRACT
UNCLAS	UNCLAS	UNCLAS	SAR

Table of Contents

I. Introduction

The realized and potential electronic applications of AlN, GaN and SiC are well known. Moreover, a continuous range of solid solutions and pseudomorphic heterostructures of controlled periodicities and tunable bandgaps from 2.3 eV (3C-SiC) to 6.3 eV (AlN) have been produced at North Carolina State University (NCSU) and elsewhere in the GaN-AlN and AlN-SiC systems. The wide bandgaps of these materials and their strong atomic bonding have allowed the fabrication of high-power, high-frequency and high-temperature devices. However, the high vapor pressures of N and Si in the nitrides and SiC, respectively, force the use of low deposition temperatures with resultant inefficient chemisorption and reduced surface diffusion rates. The use of these low temperatures also increases the probability of the uncontrolled introduction of impurities as well as point, line and planar defects which are likely to be electrically active. An effective method must be found to routinely produce intrinsic epitaxial films of AlN, GaN and SiC having low defect densities.

Recently, Ceyer [1, 2] has demonstrated that the barrier to dissociative chemisorption of a reactant upon collision with a surface can be overcome by the translational energy of the incident molecule. Ceyer's explanation for this process is based upon a potential energy diagram (Fig. 1) similar to that given by classical transition-state theory (or activated-complex theory) in chemical kinetics. The dotted and dashed lines in Fig. 1 show, respectively, the potential wells for molecular physisorption and dissociative chemisorption onto the surface. In general, there will be an energy barrier to overcome for the atoms of the physisorbed molecule to dissociate and chemically bond to the surface. Depending upon the equilibrium positions and well depths of the physisorbed and chemisorbed states, the energy of the transition state E^* can be less than zero or greater than zero. In the former case, the reaction proceeds spontaneously. In the latter case, the molecule will never proceed from the physisorbed state (the precursor state) to the chemisorbed state unless an additional source of energy can be drawn upon to surmount the barrier. This energy can only come from either (1) the thermal energy of the surface, (2) stored internal energy (rotational and vibrational) of the molecule, or (3) the incident translational kinetic energy of the molecule. Conversion of translational kinetic energy into the required potential energy is the most efficient of these processes. Moreover, by adjusting the kinetic energy, Ei, of the incoming molecule, it is possible to turn off the reaction ($Ei < E^*$), to tailor the reaction to just proceed ($Ei = E^*$), or to set the amount of excess energy to be released ($Ei > E^*$). The thrust of the present research is to employ these attributes of the beam translational energy to tune the reaction chemistry for wide bandgap semiconductor epitaxial growth.

The transition state, E^*, is essentially the activation energy for dissociation and chemisorption of the incident molecules. Its exact magnitude is unknown, but is most certainly

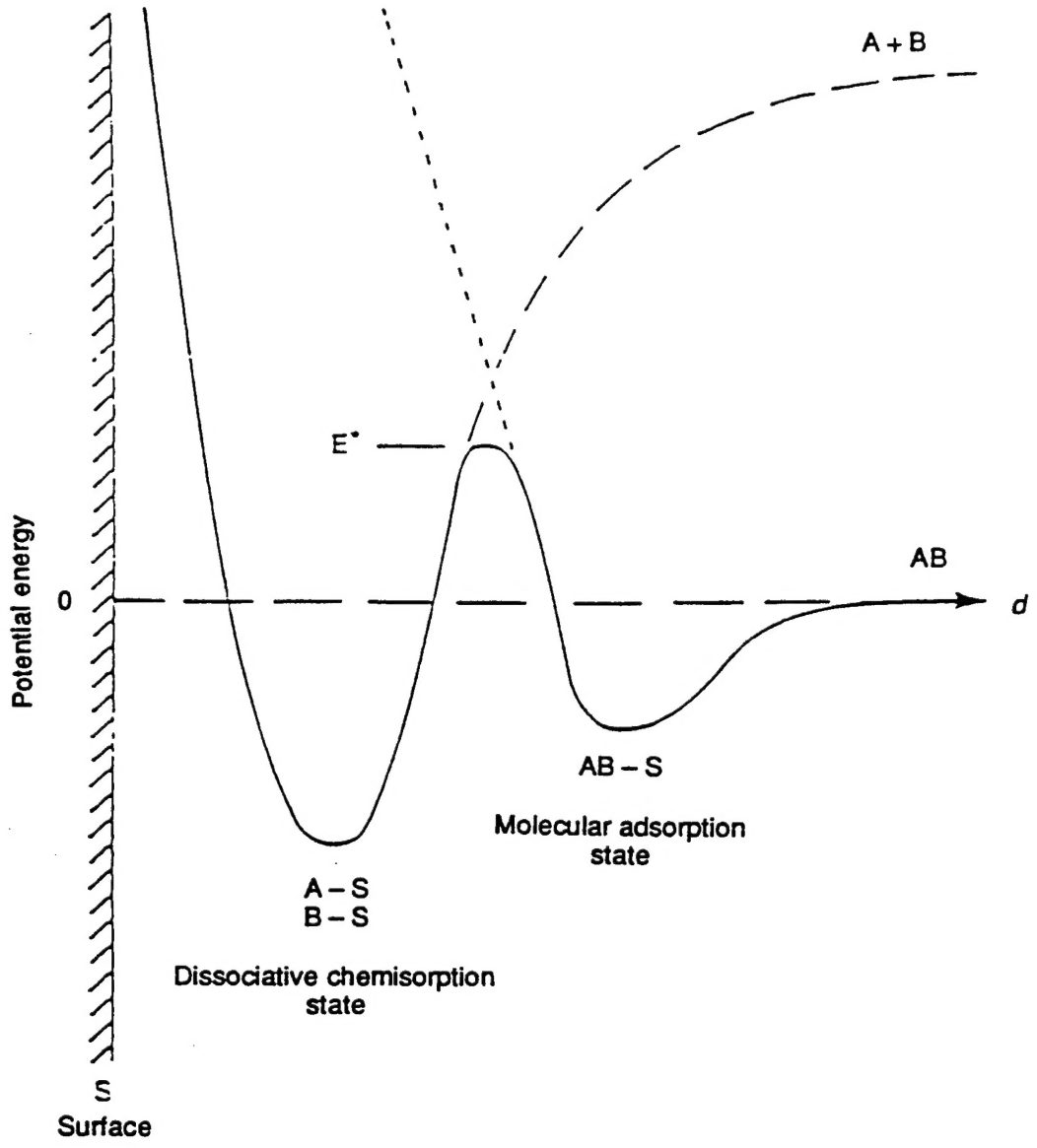

Figure 1. Schematic potential energy diagram of an activated surface reaction involving a molecularly physisorbed precursor state [from Ref. 1].

lower than the dissociation energy of the free molecule. It does not necessarily follow, however, that any kinetic energy above E* will promote high-quality epitaxial growth of GaN. One must take into consideration another energy threshold, Ed, beyond which the kinetic energy of the incident flux will cause damage to the epitaxial film being synthesized. A typical Ed threshold value is approximately five times the bandgap of the crystal and in the case of GaN, Ed ≈18 eV.

From the above consideration, it is clear that the key to high quality epitaxial growth is to be able to tune the energy of the incoming flux species over a range of energies defined by the window between E* and Ed. Since the window is quite restrictive, i.e. 1-20 eV, it is essential

that the energy spread of the flux species must be small, i.e. the flux species should ideally be monoenergetic. To this end, we employ Selected Energy Epitaxial Deposition (SEED) systems for the growth of AlN, GaN and SiC wide bandgap semiconductors. The SEED systems are of two types: (1) a seeded-beam supersonic free-jet (SSJ) and (2) a dual ion-beam Colutron. Both these SEED systems have the desirable property of a narrow energy spread of ≤ 1 eV.

Epitaxial growth using the seeded-beam SSJ involves a close collaboration between investigators at NCSU and Arizona State University (ASU). At ASU, the SSJ is interfaced directly into a low-energy electron microscope (LEEM) for the conduct of *in situ* studies of the nucleation and growth of epitaxial layers; while at NCSU, the SSJ systems are used to grow device-quality AlN, GaN and SiC for real applications. Exchanges in personnel (students) and information between the two groups ensures the achievement of desired results. The additional thin film growth experiments using dual-beam Colutrons and the theoretical studies referred to in this report are primarily conducted at ASU.

The research conducted in this reporting period and described in the following sections has been concerned with (1) modeling of the zincblende and wurtzite phases of AlN and GaN using the multicenter tight-binding method, (2) *ex situ* cleaning and etching of 6H-SiC surfaces, (3) selected energy epitaxial deposition of GaN and AlN, (4) beam characterization of dual Colutron ion-beams, and (5) approaches attempted to obtain high-quality 6H-SiC(0001) substrates for epitaxial growth of nitride films. The following individual sections detail the procedures, results, discussions of these results, conclusions and plans for future research. Each subsection is self-contained with its own figures, tables and references.

1. S. T. Ceyer, Langmuir 6, 82 (1990).
2. S. T. Ceyer, Science 249, 133 (1990).

II. *Ab initio* Calculations of the Structure and Growth Properties of the III-V Nitrides

With the extensions of the tight-binding formalism, we are now able to perform molecular-dynamics simulations for a large variety of systems on the same basis. First of all, the structural and vibrational properties of bulk III-V nitrides can be calculated with a deviation from the experimental results of only a few percent: the lattice constant and frequency of the transverse optical phonon, as well as the bulk modulus determined for cubic GaN and AlN are shown in Table I together with experimental data and the findings of the mixed-basis calculation of Miwa and Fukumoto [1] chosen representatively for other *ab initio* calculations. Table II summarizes the main results obtained for the wurtzite structure. The good agreement of the data indicates that we have a reliable basis for our further molecular dynamics simulations including carefully constructed pseudopotentials and an appropriate basis set for the expansion of the electronic charge density in terms of confined atomic orbitals. The accuracy of our method is comparable to that of highly converged *ab initio* calculations [1, 2]. However, the influence of the Ga 3*d* states is not included in the tight-binding formalism. Therefore, we obtain an underestimation of the structural parameters calculated for GaN while the differences are significantly smaller for AlN. Nevertheless, our results show the same degree of accuracy as known from previous investigations for other systems [3-6].

The next step in our studies of the growth properties of III-V consists in the investigation of interfaces and surfaces, as well as the adsorption and collision of simple molecules. Currently, we determine the atomic structure and dynamics of nonpolar low-index surfaces of III-V nitrides. By means of systematically reducing the kinetic energy, we use the dynamics of a given atomic configuration, in order to find structures of minimal total energy. We compare our results with the findings of the plane-wave calculation of Ref. [7] performed for GaN($10\bar{1}0$) and GaN($11\bar{2}0$). The agreement shown in Tables I and II for some chosen physical properties of the bulk material indicates that the density-functional tight-binding model is expected to yield accurate results also for the surfaces of GaN. Moreover, it is interesting to analyze the stability of the surface structures with molecular-dynamics simulations and to determine the interatomic force constants by means of the frozen-phonon approach.

Because of the lack of an ideal substrate for heteroepitaxy, it is important to understand the influence of the parameters given by the substrate on the growth of the cubic or hexagonal phase. We therefore calculate the structural, electronic, and dynamical properties of biaxially strained III-V-nitride semiconductors. The determination of band parameters and phonon frequencies as a function of uniaxial and biaxial strain provides information for experiments probing the properties of stressed and strained films.

Tables

Table I

Lattice constant a_0, bulk modulus B_0 and Γ-point frequency (in cm^{-1}) of the transverse-optical (TO) phonon of GaN and AlN in zincblende structure. Columns 4 and 7: results of the mixed-basis calculation of Miwa and Fukumoto (Ref. [1]).
Experimental data: [a]Reference [8], [b]Reference [9]. The experimental data for AlN are extrapolated from those of the wurtzite structure [10].

	zincblende GaN			zincblende AlN		
	present work	experiment	DFT Miwa *et al.*	present work	experiment	DFT Miwa *et al.*
a_0 (Å)	4.382	4.519[a]	4.446	4.342	4.340[c]	4.421
B_0 (MBar)	2.03	–	1.95	1.97	2.18[c]	1.95
TO	541	555[b]	558	643	–	648

Table II

Structural parameters a, c and u, bulk modulus B_0 and Γ-point frequency (in cm^{-1}) of the optical modes of GaN and AlN in wurtzite structure. Columns 4 and 7: results of the mixed-basis calculation of Miwa and Fukumoto (Ref. [1]). experimental data: [a]Reference [11], [b]Reference [12], [c]Reference [13], [d]Reference [9], [e]Reference [14].

	wurtzite GaN			wurtzite AlN		
	present work	experiment	DFT Miwa *et al.*	present work	experiment	DFT Miwa *et al.*
a (Å)	3.093	3.190[a]	3.146	3.067	3.110[a]	3.144
c (Å)	5.035	5.189[a]	5.125	4.940	4.980[a]	5.046
u	0.376	0.377[a]	0.377	0.381	0.382[a]	0.381
B_0 (MBar)	2.03	–	1.95	1.97	2.02[b]	1.95
E_2^1	191	144[c]	146	334	241[c]	228
B_1^1	321	–	335	538	–	534
A_1-TO	561	537[d]	534	619	614[e]	601
E_2^2	559	571[d]	568	647	660[e]	655
E_1-TO	557	556[d]	556	672	673[e]	650
B_1^2	726	–	697	731	–	703

Finally, we begin to investigate the collision of molecules like N_2 or NH_3 with the surface of a III-V nitride compound. Molecular-dynamics simulations allow us to follow such processes in realistic microscopic calculations. In this way, we obtain insight into possible reaction paths, the mechanism of the adsorption of an atom or the fraction of a molecule on the surface, and the collision induced dissociation of molecules. Important questions need to be answered. What energy is needed for inducing molecular dissociation and hence, chemisorption? Within what range of the collision energy can chemisorption occur without severely damaging the surface structure? Initial calculations for N_2 and NH_3 show that these molecules are reasonably well characterized within the tight-binding formalism. For N_2, we obtain a bonding distance of 1.227 Å that overestimates the experimental value that is 1.094 Å. The bonding distance between hydrogen and nitrogen calculated for ammonia amounts to 1.134 Å, while the experimental result is 1.014 Å. For the H-N-H bonding angle, we obtain 110° which is larger compared to 107° measured for NH_3.

References

1. K. Miwa and A. Fukumoto, Phys. Rev. B **48**, 7897 (1993).
2. A. F. Wright and J. S. Nelson, Phys. Rev. B **50**, 2159 (1994).
3. O. F. Sankey and D. J. Niklewski, Phys. Rev. B **40**, 3979 (1989).
4. O. F. Sankey, D. A. Drabold, and G. B. Adams, Bull. A. Phys. Soc. **36**, 924 (1991).
5. A. A. Demkov, J. Ortega, O. F. Sankey, and M. Grumbach, Phys. Rev. B **52**, 1618 (1995).
6. J. Ortega, J. P. Lewis, and O. F. Sankey, Phys. Rev. B **50**, 10516 (1994).
7. J. E. Northrup and J. Neugebauer, Phys. Rev. B **53**, R10477 (1996).
8. S. Strite and H. Morkoc, J. Vac. Sci. Technol. B **10**, 1237 (1992).
9. A. Tabata, R. Enderlein, J. R. Leite, S. W. da Silva, J. C. Galzerani, D. Shikora, M. Kloidt, and K. Lischka, J. Appl. Phys. **79**(8), 4137 (1996).
10. J. A. Sanjuro, E. Lopez-Cruz, P. Vogl, and M. Cardona, Phys. Rev. B **28**, 4579 (1983).
11. H. Schulz and K. H. Thiemann, Solid State Commun. **23**, 815 (1977).
12. K. Tsubouchi, K. Sugai, and N. Mikoshiba, *1981 Ultrasonics Symposium Proceedings* (IEEE, New York, 1981), Vol. 1.
13. P. Perlin, A. Polian, and T. Suski, Phys. Rev. B **47**, 2874 (1993).
14. L. E. McNeil, M. Grimsditch, and R. H. French, J. Am. Ceram. Soc. **76**, 1132 (1983).

III. Deposition of AlN Thin Films on Si(100) using a NH_3 Seeded He Supersonic Molecular Beam Source

A. Introduction

The nitride family of AlN, GaN and InN thin films have shown to be strong candidates for electronic and optoelectronic applications. With direct band gaps of 6.2 eV, 3.4 eV and 1.9 eV for AlN, GaN and InN respectively, solid solutions based on these materials provide for band gap modifications suitable for applications ranging from the red to the deep UV region of the spectrum [1]. Due to the high bond strength between N and H in NH_3, the growth of III-V nitrides requires high substrate temperatures unless some other form of activation is present. Supersonic Molecular Beam Epitaxy (SMBE) has been shown to enhance the surface decomposition of silane and methane [2,3] because of the possibility of tuning the kinetic energy of these species to deform and cleave the bonds upon impact with the substrate. In addition, the tuning of the energy spread is possible with SMBE. This is important in order to experimentally determine the chemisorption barriers for the systems being studied, as well as to provide species with high sticking coefficients at high enough intensities. SMBE is, therefore, a useful technique for the low-temperature growth of single-crystalline GaN films at suitable growth rates using NH_3. A review of supersonic molecular beams can be found in Scoles [4].

Deposition of AlN thin layers onto Si(100) using a triply differentially pumped NH_3 seeded He supersonic molecular beam source has been demonstrated. Preliminary results on the film stoichiometry and surface morphology are presented.

B. Experimental Procedure

The molecular beam source chamber has been described in previous reports. The source chamber was interfaced with a deposition chamber which houses a sample holder, an isolation valve between the source and the deposition chamber and an Al evaporator. The deposition chamber was pumped by a liquid nitrogen trapped M-4 Varian diffusion pump. The samples were resistively heated by passing a current through them and the temperature was measured using a disappearing filament pyrometer. The temperature of the Al evaporator was also measured with the pyrometer. In the present study, the substrates were B-doped Si(100) (resistivity = 0.09 Ωcm) wafers. The substrates were degreased by rinsing and sonicating in methanol and acetone. The samples were then loaded into the deposition chamber and the chamber was evacuated and baked such that a base pressure $< 5\times10^{-9}$ Torr is obtained. A liquid nitrogen trap was then filled to obtain a base pressure $< 3\times10^{-10}$ Torr. The filament surrounding the BN crucible containing Al was degassed by heating it until a pressure of 6×10^{-10} Torr was obtained with the filament at 900°C. The sample was then degassed by heating to 650°C while the pressure in the chamber was maintained at $< 1\times10^{-9}$ Torr. At this

point, the sample was flashed to 1150°C three times for a period of 10 seconds each. The sample was then cooled to the deposition temperature and a layer of Al was evaporated on it. At this point the isolation valve between the source chamber and the deposition chamber was opened such that the NH_3 seeded He beam impinged on the sample. After the deposition was completed the Al shutter was closed, the evaporator was turned off and the sample was progressively cooled in the presence of the NH_3 seeded He beam. The samples were then characterized for composition and surface morphology using Rutherford Backscattering Spectroscopy (RBS) channeled along the Si [110] direction and Nomarski optical microscopy. Preliminary runs at a substrate temperature of 785°C and 1000°C have been completed under varying Al fluxes. The NH_3 beam intensity was 1×10^{16} $cm^{-2}s^{-1}$, the deposition time was 45 min., the stagnation temperature was 300K for a NH_3 energy of ≈ 0.22eV, and the nozzle diameter was 100μm at a stagnation pressure of 820 Torr.

C. Results and Discussion

Figure 1(a) shows the RBS spectra for sample #1 deposited at a substrate temperature of 1000°C and Al evaporator temperature of 1200°C. Tungsten contamination on the film was due to the filament being evaporated, however it is less than 0.5% W. It is important to note that the yield detected for a certain element in RBS scales with the atomic number of the element squared. The stoichiometry of the film as derived from the spectra indicates some excess Al. This is in part due to the Al and Si signal appearing at the same energy and the RBS beam sampling outside the area covered by the NH_3/He molecular beam during deposition. We are in the process of performing Auger Electron Spectroscopy to confirm the composition of the sample. A second sample (#2) was deposited at 785°C under the same conditions as mentioned above and showed Al droplets on the surface. By lowering the evaporator temperature to 1150°C a nearly stoichiometric film (#3) was obtained at 785°C as shown in Fig. 1(b). The source of O contamination might be due to excess Al being oxidized or the native oxide formed on exposed Si substrate which was not covered totally by the AlN layers. However, as mentioned previously further analysis of the samples is required. The normalized yield seems to be close for both RBS spectra suggesting that the films are of similar thickness (≈100Å).

Images of the deposited films taken with the Nomarski optical microscope show rough surfaces with irregularly shaped features.

D. Conclusion

Deposition of AlN films with NH_3 seeded He supersonic molecular beams on Si(100) has been demonstrated at 1000°C and 785°C. Further studies to confirm the stoichiometry of the samples are under way. The fact that growth was obtained under ultrahigh vacuum at a rate of ≈ 1ML/min indicates that deposition in the LEEM is feasible.

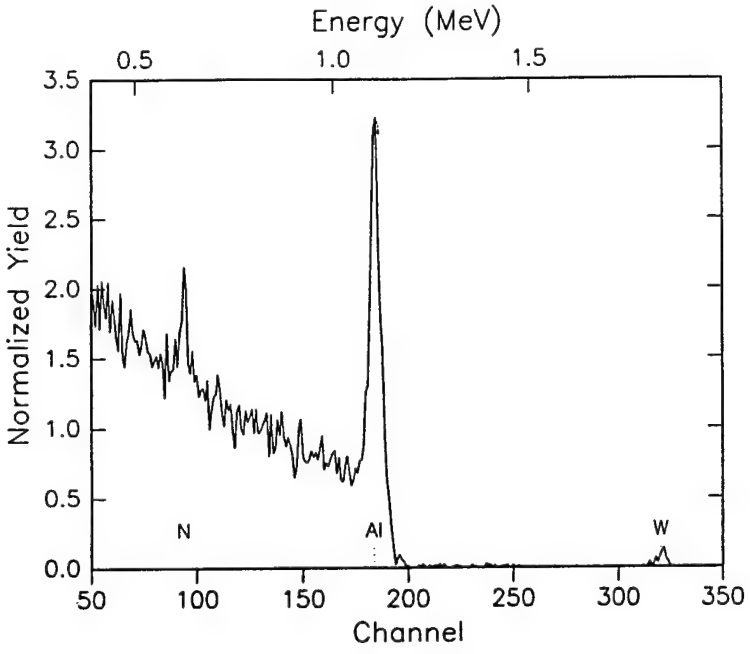

Figure 1(a). Sample #1 RBS spectra, substrate temp. of 1000°C and Al evaporator temp. of 1200°C.

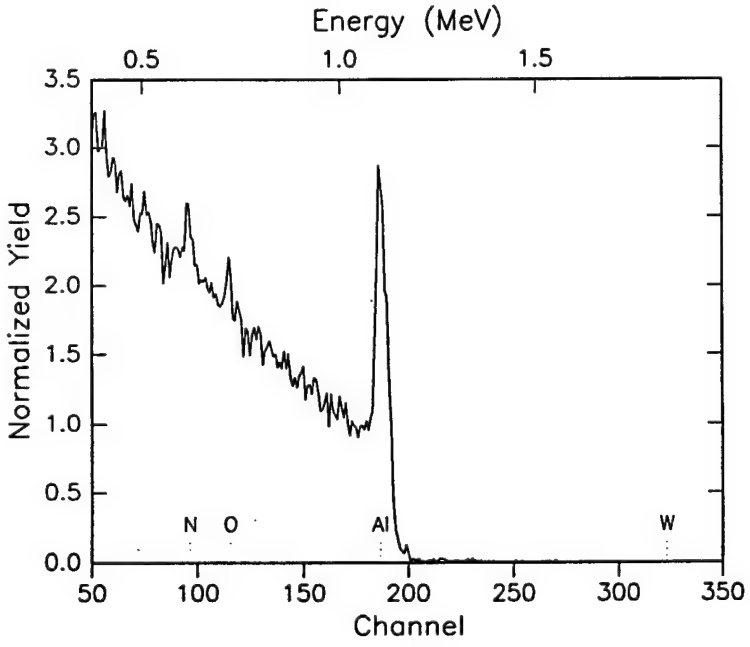

Figure 2(a). Sample #3 RBS spectra, substrate temp. of 785°C and Al evaporator temp. of 1150°C.

E. Future Work

Further study of the relationship between the sample temperature and the Al flux will be conducted. Preliminary depositions of GaN will be attempted.

F. References

1. S. Strite and H. Morkoc, J. Vac. Sci. Technol. **B10**, 1237 (1992).
2. M. E. Jones, L. Q. Xia, N. Maity, J. R. Engstrom, Chem. Phys. Lett. **229**, 401 (1994).
3. S. T. Ceyer, J. D. Beckerle, M. B. Lee, S. L. Tang, Q. Y. Yang, M. A. Hines, J. Vac. Sci. Technol. A **5**, 501 (1987).
4. D. R. Miller, *Atomic and Molecular Beam Methods*, Ch. 2, Ed. G. Scoles, Oxford University Press (1988).

IV. Selected Energy Epitaxial Deposition (SEED) of III-V Nitride and SiC Thin Films

A. Introduction

Gallium nitride is a wide bandgap semiconductor (E_g = 3.4 eV) with great potential for optoelectronics and high-temperature, high-frequency, microelectronics applications. State-of-the-art GaN films ($\leq 10^8$ defects per cm^2) have been used to fabricate blue light emitting diodes (LEDs) and laser diodes. Moreover, GaN forms a continuous range of solid solutions with AlN (6.28 eV) and InN (1.95 eV), permitting the fabrication, via bandgap engineering, of laser diodes with tunable emission frequencies from covering the visible and UV regions.

Heteroepitaxial growth of high-quality monocrystalline GaN films has been problematic due to the lack of a suitable lattice-matched substrate and the thermodynamic instability of GaN under high-temperature, low-pressure chemical vapor deposition (CVD) conditions. Sapphire, the most common substrate, exhibits a 16% lattice mismatch at the GaN(0001)/sapphire(0001) interface; moreover, the thermal expansion coefficient of sapphire is 25% greater than that of GaN. Only by employing a low-temperature AlN or GaN buffer layer can one obtain monocrystalline films on sapphire with defect densities in the 10^8-10^9 cm^{-2} range.

Substrate temperatures in excess of 1000°C are required for growth of monocrystalline GaN films by halide or metal-organic CVD using NH_3. Substrate thermal energy is required to overcome the activation barriers for dissociative chemisorption of NH_3 and adatom surface migration (lateral diffusion). Such high growth temperatures are undesirable as GaN is thermally unstable above 620°C *in vacuo* [1]. Plasma-assisted processes have been utilized to lower the GaN growth temperature to approximately 700°C, but ion-induced damage and oxygen contamination are often observed.

The use of energetic neutral beams of precursor molecules is an alternative approach to the epitaxial growth of GaN films at lower substrate temperatures. In selected energy epitaxy (SEE), heavy reactant molecules are seeded in a supersonic expansion of light molecules and thereby accelerated to hyperthermal energies. The precursor molecules attain kinetic energies on the order of several eV which can provide the necessary energy for activated surface processes, such as dissociative chemisorption and adatom migration. Hence, in prospect, monocrystalline GaN films may be grown at much lower substrate temperatures by SEE than by conventional thermal techniques [2]. Moreover, energetic neutral beams with narrow energy distributions are useful in fundamental studies of wide bandgap semiconductor growth using *in situ* low-energy electron microscopy (LEEM) and other techniques.

As discussed in previous reports (Sept. 1995, Dec. 1995, Mar. 1996), GaN thin films have been deposited on sapphire(0001) via SEE at 600°C using V/III ratios ≥200. From these results, it is evident that incident translational energies of the precursors, NH_3 and

triethylgallium (TEG), in the hyperthermal regime do influence GaN growth kinetics and film morphology. However, a two-step growth sequence involving low-temperature deposition of a buffer layer followed by growth at higher temperatures was required to achieve smooth, highly-oriented GaN films on sapphire(0001).

Nitridation of sapphire using NH_3 or plasma-generated nitrogen species has been reported to improve the quality of subsequently deposited III-nitride films.[3] A thin AlN_xO_{1-x} layer has been shown to promote 2D growth, apparently by decreasing the interfacial free energy between the GaN film and the substrate. The success of this approach suggested to us that nitridation of GaP might provide a suitable buffer layer for nucleation and growth of GaN. Moreover, GaP(001) might be a useful surface for future N sticking coefficient measurements using hyperthermal NH_3 beams. GaP(001) has been used as substrate for growth of α- and β-GaN [4,5]. In this report, we examine *ex situ* cleaning procedures for GaP and *in situ* nitridation using active nitrogen species from a remote RF N_2 plasma. Experimental details of our first, albeit unsuccessful, attempts at GaN growth on Si(100) using dual seeded supersonic beams of TEG and NH_3 are also described.

B. Experimental Methods

Selected Energy Epitaxy of GaN. Preliminary beam characterization and growth experiments were done using the new multi-chamber SEE system described in the previous report. The apertures used for TEG and NH_3 nozzles were 50 and 150 μm in diameter, respectively. The NH_3 and TEG nozzle temperatures were maintained at 680 and 80°C, respectively, during growth and beam characterization.

Table I illustrates the dependence of the NH_3 nozzle stagnation pressure on the flow rates of He and NH_3. Table II contains similar data for the TEG nozzle; here, the TEG bubbler temperature was maintained at 0°C.

Table I. Experimental Stagnation Pressure-Flow Relationship for NH_3 Nozzle

He flow rate (sccm)	NH_3 flow rate (sccm)	Stagnation pressure (Torr)
200	10	300
300	15	440
400	15	560
700	15	890

Table II. Experimental Stagnation Pressure-Flow Relationship for TEG Nozzle

He flow rate (sccm)	Stagnation pressure (Torr)
10	150
60	870

Mass spectra of the NH_3 and TEG beams were measured at the sample position using the Hiden HAL/3F 301 PIC quadrupole mass spectrometer (QMS). The NH_3 flow rate was 5 sccm, and the nozzle-to-skimmer distance was 2 mm. For TEG, the He flow rate was 5 sccm, and the bubbler temperature was 10°C. The QMS settings were as follows: electron energy, 70 eV; emission current, 50 μA; cage voltage, 3 V; focus, -90 V; multiplier voltage, 1800 V.

Preliminary GaN SEE conditions are given in Table III; hydrogen-terminated Si(100) wafers were used as substrates.

Table III. Conditions for Preliminary GaN Growth Experiments

TEG nozzle	50 μm in diameter
TEG nozzle temperature	80°C
TEG bubbler temperature	0°C
TEG pressure (estimated)	0.8 Torr
He carrier gas flow	10 sccm
stagnation pressure at TEG nozzle	150 Torr
NH_3 nozzle	150 μm in diameter
NH_3 nozzle temperature	680°C
NH_3 flow rate	5 sccm
He flow rate	100 sccm
Stagnation pressure at NH_3 nozzle	160 Torr
Growth chamber pressure	1.6E-5 Torr
Growth temperature	600°C

The base pressures of the growth chamber and differential pumping chamber were less than 3E-8 Torr and 3E-7 Torr, respectively.

In order to facilitate time-of-flight (TOF) velocity measurements on seeded supersonic beams, a rotating disk chopper and chopper motor driver circuitry were designed and fabricated. The chopper consists of a 4-in. stainless steel disk with two 1-mm teeth at 180° angles. Two choppers can be mounted on a custom-fabricated frame (Figure 1) in the second differential pumping stage of the SEE system. The height of each chopper can be adjusted to ensure proper beam alignment. The choppers may be rotated at up to 400 Hz (24000 rpm) using 3-phase synchronous motors (Globe, B2000). The motor driver circuitry was built using a design provided by Professor James Engstrom of Cornell University. The design employs a function generator, power supply and necessary digital circuitry to convert a 0.4-2 kHz square-wave input into a 3-phase output to driven the chopper motor.

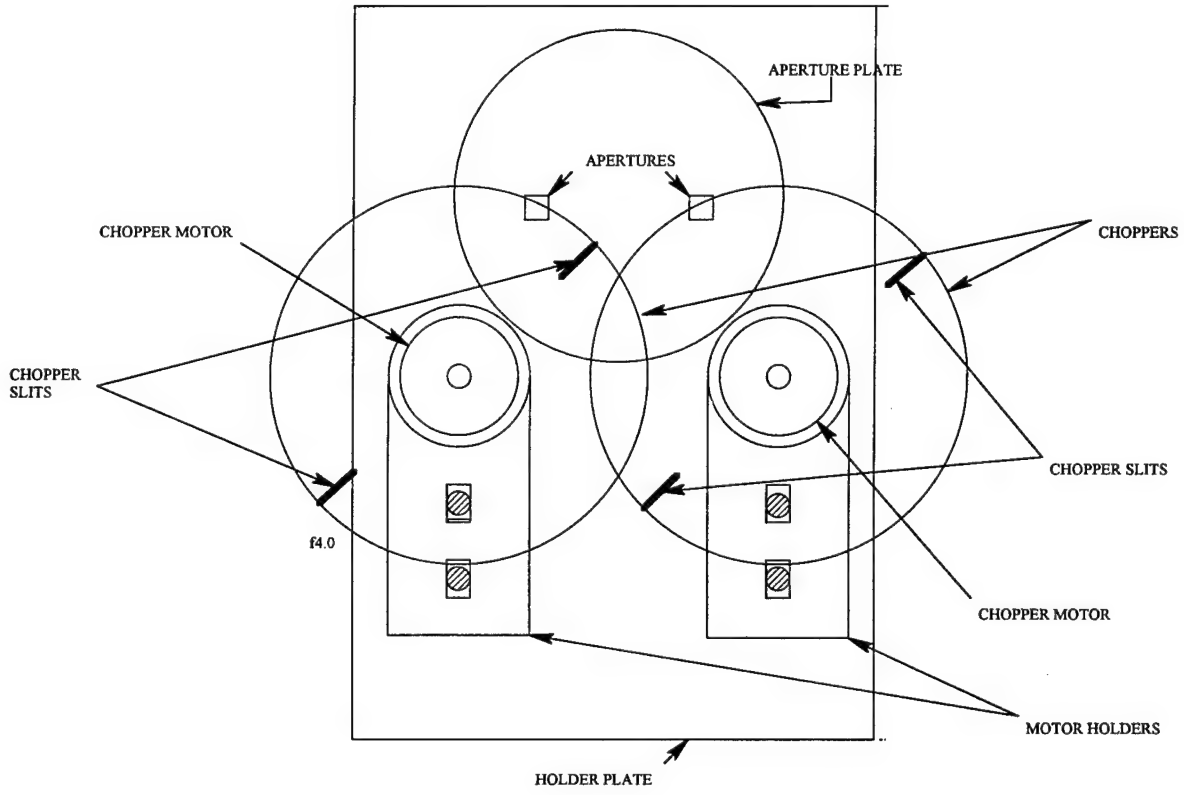

Figure 1. Schematic of Rotating Disk Choppers and Collimating Apertures

Ex-situ Cleaning of GaP. Samples (5×7 mm^2) cleaved from a GaP(100) wafer were subjected to combinations of UV/ozone (O_3) cleaning and standard wet chemical treatments. UV/O_3 cleaning consisted of exposing the sample to UV radiation and in-situ generated O_3 from low-pressure Hg vapor lamp operating in air; samples were exposed for 10 min on each side to remove hydrocarbons and grow a thin photochemical oxide layer. Following the

subsequent wet chemical steps, the samples were rinsed in DI water (18 MΩ-cm) for 2 min and blown dry with nitrogen. After cleaning, samples were introduced to a UHV surface analysis chamber via an oil-free, cryo-pumped loadlock; surface analyses were performed using either Auger electron spectroscopy (AES) and low-energy electron diffraction (LEED) or x-ray photoelectron spectroscopy (XPS). In some cases, a UHV anneal was performed employing radiant heating of the sample from the backside using a W filament. In a typical anneal, the sample was heated to 800°C in 15 min and then allowed to cool gradually to 25°C prior to surface analysis.

Details of the wet chemical treatments are as follows:

1. HCl clean: The sample was dipped in electronic grade HCl (38%) for 1 min at 25°C.
2. H_3PO_4 clean: The sample was dipped in H_3PO_4 (85%) for 10 s at approximately 100 °C.
3. H_3PO_4/H_2SO_4 clean: The sample was dipped in a 1:1 mixture of 85% H_3PO_4 and concentrated H_2SO_4 for 20 s at approximately 100°C.

Remote Plasma Nitridation of GaP: Typically, *ex situ* cleaned GaP(100) samples were exposed to a remote RF N_2 plasma (100 mTorr, 100 sccm N_2, 25 W) at 200°C for 5 min. HCl-cleaned samples were nitrided at 100-400°C to study the effect of temperature on surface composition and nitride layer thickness. One sample was nitrided for 15 min at 200°C.

C. Results and Discussion

GaN SEE. The mass spectrum of TEG seeded in He measured at the sample position is shown in Fig. 2. Peaks due to Ga isotopes are observed at 69 and 71 m/e. Peaks due to diethyl gallium, DEG, (m/e=127,129) and monoethyl gallium hydride, MEGH, (m/e=99, 101) are readily detected. As expected, the signals from the TEG parent ion (m/e = 156, 158) are extremely weak. The strong peaks near mass-to-charge ratios of 18 and 28 are due to background water and fragments of the ethyl ligands, respectively.

We demonstrated that molecular beams of source compounds could be injected into the growth chamber. The first GaN growth experiments were performed using dual seeded supersonic beams of NH_3 and TEG. Unfortunately, the initial experiments using hydrogen-passivated Si(100) substrates at 600°C did not result in film growth. Our experience indicates nucleation and growth of GaN on Si is more difficult than on sapphire. We are currently refocusing our efforts on GaN growth on sapphire(0001) using a two-step nucleation/growth process.

Ex situ cleaning of GaP. Figure 3 presents AE spectra taken after each step during the HCl cleaning procedure; the derivative spectra were normalized using the Ga *LMM* peak intensities. The "native surface" of air-exposed GaP(100) consists of an oxide layer contaminated by adventitious carbon (Fig. 3a). The atomic fractions of the individual elements were estimated

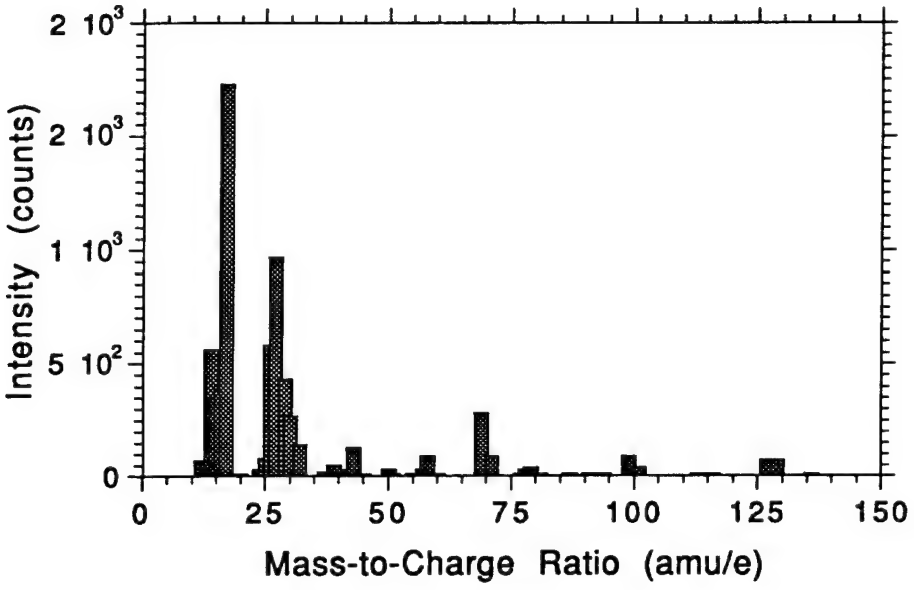

Figure 2. Mass spectrum of TEG beam in growth chamber.

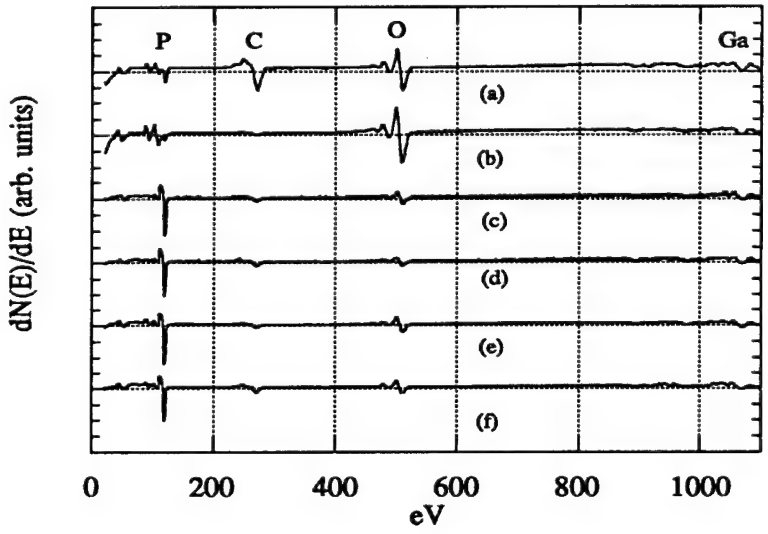

Figure 3. AE spectra of GaP: (a) native surface; (b) after UV/O_3 treatment; (c) after UV/O_3 + HCl dip; (d) after (c) and 800°C annealing; (e) after UV/O_3 + H_3PO_4 dip; (f) after (e) and 800°C annealing.

from the respective peak heights and are listed in Table I. For the native surface, the measured Ga:P ratio is 1:0.4. After UV/O_3 cleaning, the carbon content is reduced by almost a factor of 6, while the oxygen content nearly doubles (Table I); the Ga:P ratio increase to 1:0.6. As can be observed in Fig. 3c, an HCl dip is effective at removing the photochemical oxide layer; however, the carbon content is found to increase by almost a factor of 2. After the HCl dip, the surface is phosphorus rich (Ga:P = 1:1.4) and a dim LEED pattern can be observed using

electron beam energies of 132 eV and higher. A small amount of chlorine is also detected on the surface. Subsequent annealing of this sample at 800°C in a UHV environment results in slight reductions of the carbon and oxygen concentrations (Fig. 3d). The phosphorous level on the surface is found to increase marginally (< 10%), possibly due to the diffusion of phosphorous from the bulk to the surface at high temperatures. LEED patterns are still observed at similar electron beam energies.

Table IV. Elemental Compositions of GaP Surfaces

Surface Treatment	atom% Ga	atom% P	atom% 0	atom% C	atom% Cl/S
None (native)	24	10	7	44	-
UV/O_3	27	17	47	8	-
UV/O_3 + HCl	29	41	13	17	1.7 (Cl)
UV/O_3 + HCl + anneal	31	45	9	14	0.5 (Cl)
UV/O_3 + H_3PO_4	26	45	16	14	-
UV/O_3 + H_3PO_4 + anneal	26	40	14	20	-
H_3PO_4 /H_2SO_4	28	29	13	19	11 (S)

On cleaning GaP using H_3PO_4, higher concentrations of P and O are observed on the surface than after cleaning with HCl (Fig. 3e). The resultant Ga:P ratio is 1:1.7 (Table IV). Heating the sample to 800°C results in partial removal of both P and O (Fig. 3f), reducing the Ga:P ratio to 1:1.5. In contrast, heating the sample to 550°C *in vacuo* had increased the P surface concentration, while removing oxygen. LEED patterns are observed for the annealed surface at 135 eV and higher. Finally, cleaning GaP using a H_3PO_4:H_2SO_4 mixture resulted in a surface Ga:P ratio of 1:1 with substantial S contamination (Table IV).

XP spectra of GaP surfaces after various chemical treatments are presented in Fig. 4. The spectra are normalized with respect to the Ga_{3d} peak at 19 eV and calibrated with respect to the C_{1s} peak at 284.6 eV. After UV/O_3 cleaning (Fig. 4b), the O_{1s} peak at 531 eV indicates the presence of Ga and P oxides. Consistent the above AES results, XPS (Fig. 4c) indicates that HCl cleaning at 25°C is effective at removing the photochemical oxide layer; chlorine on GaP is difficult to detect by XPS due to overlap of the Cl and P photoelectron peaks. In contrast to the AES results, the XPS data indicate that H_3PO_4 at 100°C is slightly more effective than HCl at removing oxide from the GaP surface. The differing results may arise from the relative surface sensitivities of the two techniques: AES is sensitive to only the outermost atomic layers (5-10Å), whereas the XPS sampling depth is on the order of 40Å. After HCl and H_3PO_4 cleaning, the P_{2p} peak is observed at 129 eV which indicates the presence of only phosphide bonds and no phosphate bonds (133 eV).

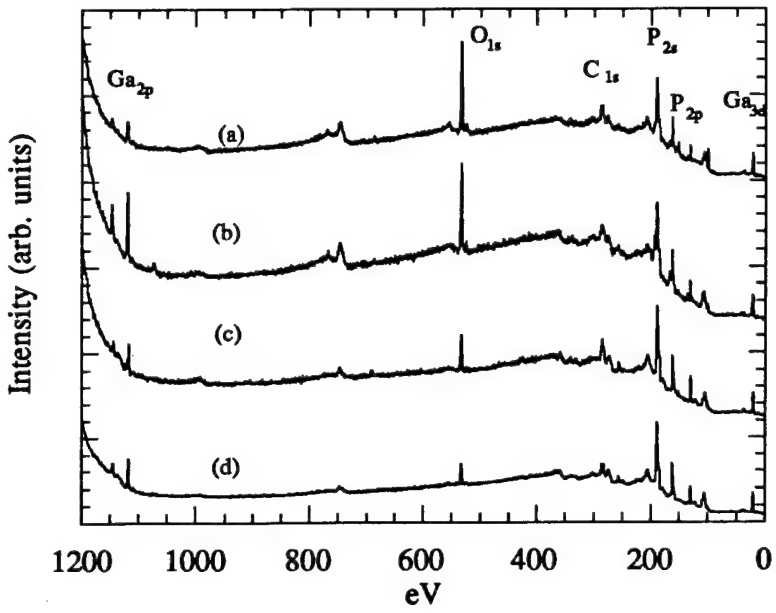

Figure 4. XP spectra of GaP: (a) native surface; (b) after UV/O_3 treatment; (c) after UV/O_3 + HCl dip; (d) after UV/O_3 + H_3PO_4 dip.

Remote Plasma Nitridation of GaP. The effects of substrate temperature and time of exposure to a remote RF N_2 plasma on GaP nitridation are illustrated in Fig. 5. The AE spectra are normalized with respect to the Ga *LMM* peaks. The plasma exposure time for each sample was 5 min, except for the sample of Fig. 5d for which it was 15 min. The plasma-generated active nitrogen species are observed to replace surface phosphorous atoms and in most cases to effectively remove adventitious carbon. *Ex situ* XPS spectra (not shown) contain N_{1s} peaks at 398.1 eV which are consistent with the formation of Ga-N bonds. The surface GaN layer is amorphous, as no LEED pattern could be observed. The stoichiometries of the nitrided layers, as determined by AES, are given in Table V. The highest nitrogen concentrations are observed at 200°C, where the Ga:N ratio is 1:1.7 for a 5-min exposure. On increasing the exposure time to 15 min, the Ga:N ratio increases to 1:1.95. The differences in nitrogen concentration over the 200-400°C temperature range, however, are not large, consistent with a weakly activated surface process. The position and line shape of the C *KLL* peak arising from residual carbon on the sample nitrided at 400°C is unusual and cannot be readily assigned to the common amorphous, graphitic or carbidic forms. We speculate that a small amount of "carbon nitride" may have formed by reaction of activated nitrogen species with adventitious carbon.

D. Conclusions

Ex situ cleaning procedures for GaP have been investigated. Both HCl and H_3PO_4 have been found to be effective in removing oxide layers created during UV/O_3 treatment. Growth of GaN layers on GaP by using a remote RF N_2 plasma was investigated. Our results suggest

that the process, which results in substitution of nitrogen for phosphorus in the outermost atomic layers, is only weakly sensitive to temperature. Remote N_2 plasma exposure is also effective in removing adventitious carbon and to some extent, oxygen.

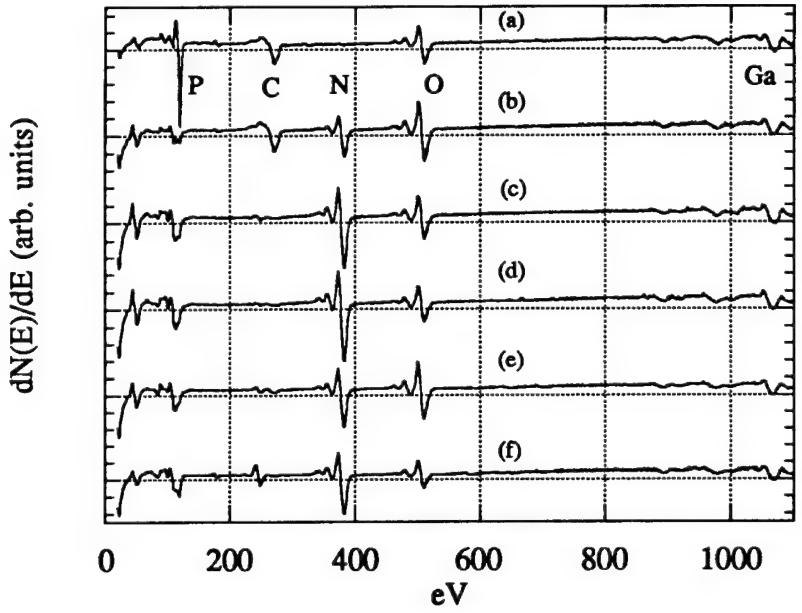

Figure 5. AE spectra of GaP exposed to nitrogen plasma at different temperatures: (a) *ex situ* cleaned; (b) 100°C; (c) 200°C; (d) 200°C (15 min.); (e) 300°C; (f) 400°C.

Table V. Surface Compositions of GaP Samples after Exposure to an RF N_2 Plasma[a]

Substrate Temperature(°C)	atom% Ga	atom% P	atom% N	atom% O	atom% C
100	22	5	22	22	28
200	26	10	45	15	4
200[b]	26	10	50	13	2
300	25	10	37	22	7
400	22	10	36	10	21

[a]Exposure times are 5 min except as noted.
[b]Exposure time was 15 min.

E. Future Plans

GaN deposition experiments are planned using dual seeded supersonic beams. Complete studies will be conducted on nitridation of GaP by nitrogen plasma from a remote RF source. Investigation will be carried out on surface reaction pathways in GaN epitaxial growth using FTIR spectroscopy.

F. References

1. S. Nakamura, Japan J. Appl. Phys. **30**, L1705 (1991).
2. M. R. Lorenz and B. B. Binkowski, J. Electrochem Soc. **109**, 24 (1962).
3. K. Uchida, *et al.*, J. Appl. Phys. **79**, 3487 (1996) and references therein.
4. T. S. Cheng, L. C. Jenkins, S. E. Hooper, C. T. Foxon, J. W. Orton and D. E. Lacklison, Appl. Phys. Lett. **66**, 1509 (1995).
5. L. C. Jenkins, T. S. Cheng, C. T. Foxon, S. E. Hooper, J. W. Orton, S. V. Novikov and V. V. Tret'yakov, J. Vac. Sci. Technol. B **13(4)**, 1585 (1995).

V. Dual Colutron Ion-Beam Deposition

We are still in the process of aligning the various components in the two low-energy ion-beam systems. When a keV ion beam is decelerated to a few eV's, space charge becomes a big problem and beam alignment must be as precise as possible to eliminate scattering and charging caused by the beam striking exposed surfaces. Thus far, we have succeeded in obtaining Ar^+, N_2^+, N^+, and C^+, ion beams at energies 10-20 eV with current densities ~200 nA cm^{-2}, corresponding to a deposition rate of ~10^{-3} MLs^{-1}. The energy distribution of the Ar^+ ions at 20 eV measured by the electrostatic energy analyzer (ESA) is shown in Fig. 1. The FWHM is ~3 eV. Most of the broadening is due to multiple scattering of the ions from surfaces before entering the ESA. With suitable alignment of the ion beam, we expect to achieve a FWHM of <1 eV in the energy distribution.

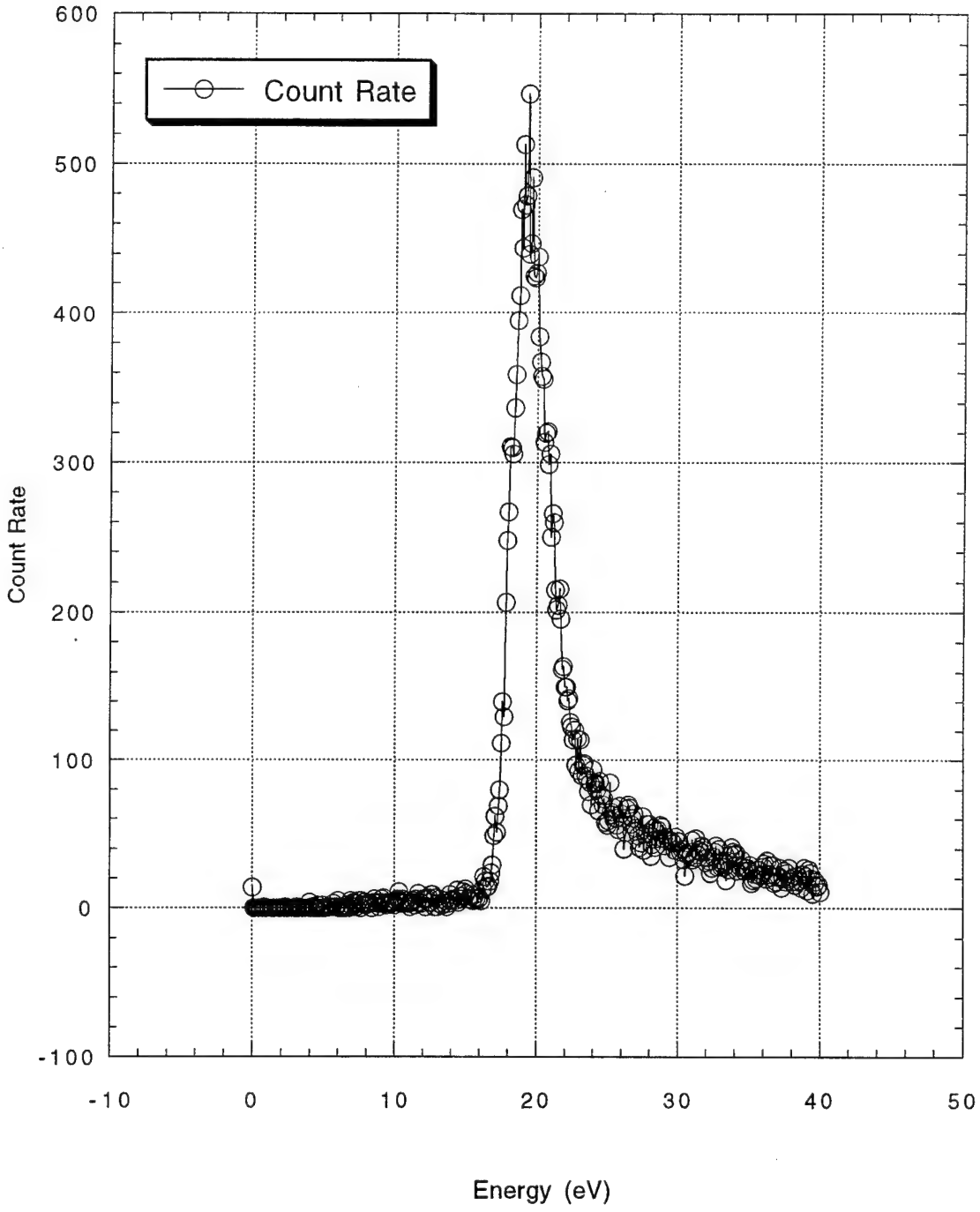

Figure 1. **Energy distribution of an Ar^+ ion beam at 20 eV.**

VI. Surface Morphology of 6H-SiC(0001) Substrates Prepared for Nitride Film Growth

A. *Ex situ* Treatment

Various *ex situ* etching procedures described in previous reports have not led to the desired result of minimizing the surface defects in commercially available SiC. In order to conduct useful growth studies in the LEEM, these defects must be minimized. However, the NASA Lewis Research Center etch process (see December 1995 report) has given the most encouraging results. Samples treated by this process have been examined in the LEEM to ascertain their suitability in future experiments and the results look promising. Figures 1 and 2 show LEEM images of 6H-SiC(0001) surfaces after etching treatment II from NASA Lewis. Additional samples will be sent to NASA Lewis for further etch studies.

B. *In situ* Treatment

In addition to *ex situ* treatments, *in situ* surface preparation procedures must be established under UHV conditions to allow useful studies by LEEM. To reach this goal, various procedures have been studied in our UHV STM's with the operating doctrine that what will produce a high-quality reconstructed surface in the STM will do so in the LEEM. In addition, operating problems with the various procedures can be dealt with before introduction into the LEEM.

SiC Surface Preparation by the Use of a Si Evaporator. The use of a Si evaporative source in the cleaning of the SiC surface in UHV STM is generally accepted. Surface steps observed are similar to that seen in Fig. 3. Various surface reconstructions have been observed depending on the sample temperature. We have tried alternative approaches.

SiC Surface Preparation by the Use of Atomic Hydrogen. One of the problems involved with the thermal cleaning of 6H-SiC in UHV is the formation of a (6×6) reconstruction that has been associated with a graphite surface. It is know that atomic hydrogen will etch graphite, thus it was hoped that by providing a flux of atomic hydrogen during the thermal cleaning a high-quality surface could be achieved. This technique, however, was not successful.

SiC Surface Preparation by the Use of Silane. The use of silane for the surface preparation of SiC in wide band-gap III-V MBE has been successful. We have been experimenting with its use to clean the surface of SiC to the standard of UHV-STM imaging, at low temperatures (850-1100ºC), and to try to emulate the results achieve to date with Si evaporation techniques.

The parameter space of time, temperature, and pressure is a large one, but we have been able to observe atomic steps on a clean surface with the parameters of 5minutes, 1100ºC, and at a pressure of 5.0E-6 Torr, see Fig. 3. Unfortunately, we have not been able to obtain atomic resolution of any surface reconstructions on these samples, and we are endeavoring to determine why this is the case. In the mean time we will continue to explore the parameter space to determine operating condition that will lead to apparently clean surfaces with atomic steps.

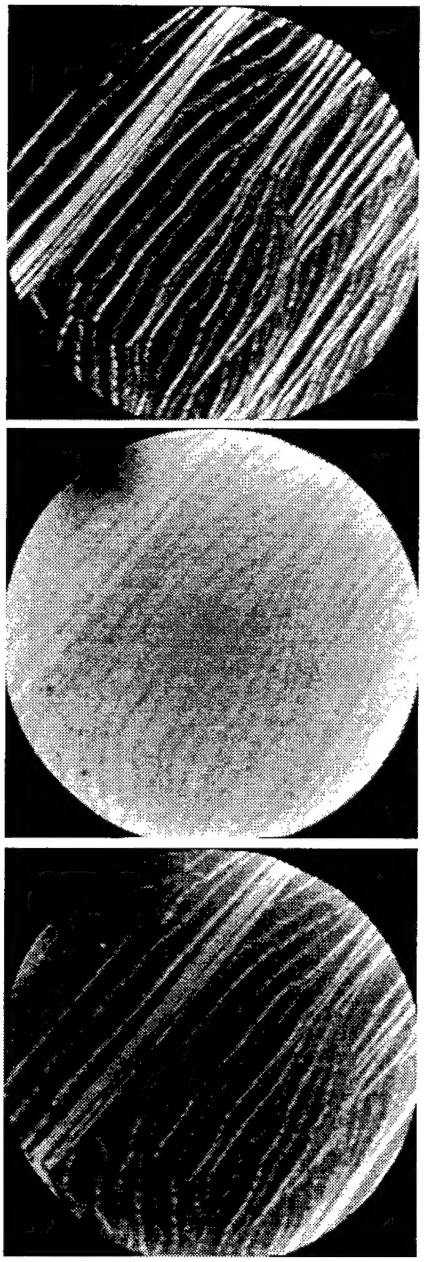

(a)

(b)

(c)

Figure 1. LEEM images from nominally a single 7μm-diameter area from the 6H-SiC(0001) surface received NASA Lewis' treatment-II, revealing the energy dependent step contrast. The electron energies are (a) 14.2 eV; (b) 24.6 eV; (c) 30.0 eV.

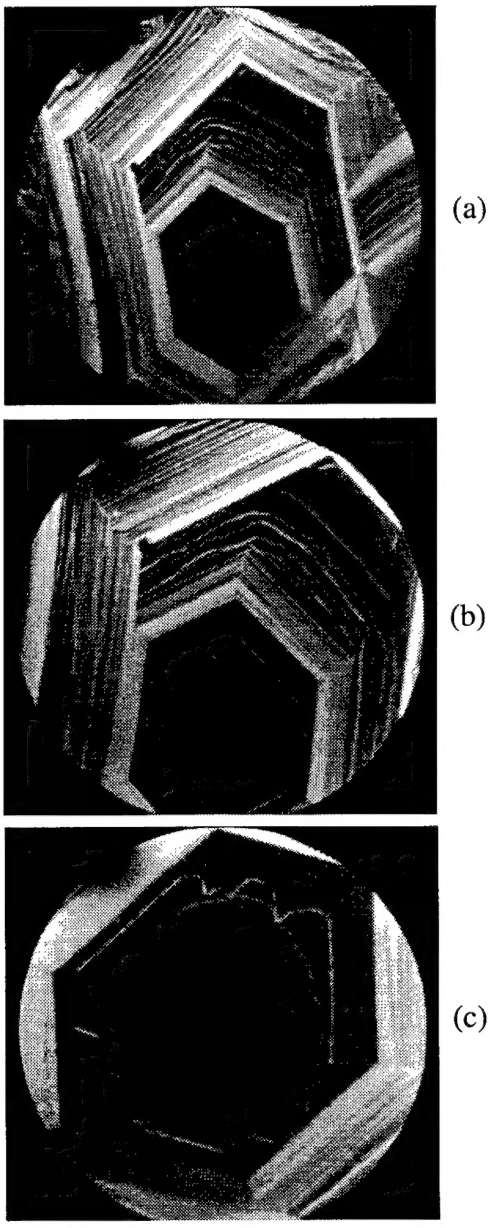

Figure 2. LEEM images of a large etch pit on the 6H-SiC(0001) surface received NASA Lewis' treatment-II. The electron energy is 6.2 eV. The fields of view are (a) 17μm; (b) 11.5μm; (c) 7μm.

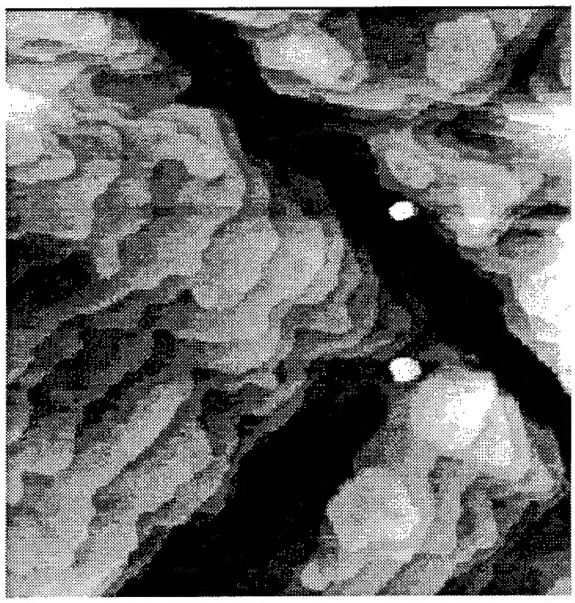

(a)

(b)

Figure 3. (a) 1000nm scan at -5.0V sample bias, at 0.5nA after silane cleaning. (b) 500nm scan at -5.0V sample bias, at 0.5nA after silane cleaning.

VII. Distribution List

Mr. Max Yoder Office of Naval Research Electronics Division, Code: 312 Ballston Tower One 800 N. Quincy Street Arlington, VA 22217-5660	3
Administrative Contracting Officer Office of Naval Research Regional Office Atlanta 101 Marietta Tower, Suite 2805 101 Marietta Street Atlanta, GA 30323-0008	1
Director, Naval Research Laboratory ATTN: Code 2627 Washington, DC 20375	1
Defense Technical Information Center 8725 John J. Kingman Road, Suite 0944 Ft. Belvoir, VA 22060-6218	2